

1 Risk of multiple interacting tipping points should encourage rapid CO₂ emission
2 reduction

3 Yongyang Cai^{1,2*}, Timothy M. Lenton^{3*}, Thomas S. Lontzek^{4*}

4 *All authors contributed equally to this work

5 ¹Hoover Institution, Stanford University, Stanford, CA 94305, USA

6 ²Becker Friedman Institute, University of Chicago, Chicago, IL 60636, USA

7 ³College of Life and Environmental Sciences, University of Exeter, Exeter EX4 4QE, UK

8 ⁴Department of Quantitative Business Administration, University of Zurich, 8008 Zürich, CH

9 **Evidence suggests that several elements of the climate system could be tipped into a**
10 **different state by global warming, causing irreversible economic damages. To address**
11 **their policy implications, we incorporated five interacting climate tipping points into a**
12 **stochastic-dynamic integrated assessment model, calibrating their likelihoods and**
13 **interactions on results from an existing expert elicitation. Here we show that combining**
14 **realistic assumptions about policymaker's preferences under uncertainty, with the**
15 **prospect of multiple future interacting climate tipping points, increases the present**
16 **social cost of carbon (SCC) in the model nearly 8-fold from \$15/tCO₂ to \$116/tCO₂.**
17 **Furthermore, passing some tipping points increases the likelihood of other tipping**
18 **points occurring to such an extent that it abruptly increases the social cost of carbon.**
19 **The corresponding optimal policy involves an immediate, massive effort to control CO₂**
20 **emissions, which are stopped by mid-century, leading to climate stabilization at <1.5 °C**
21 **warming above pre-industrial levels.**

22 The social cost of carbon (SCC) represents the cost of all future climate damages stemming
23 from a marginal emission of CO₂, discounted to the year of emission. The 2010 US Federal
24 assessment¹ used three simple integrated assessment models (IAMs) to arrive at a SCC of
25 \$21/tCO₂ for a tonne emitted in 2010, which was subsequently revised upwards² to \$33/tCO₂.
26 Several other studies³⁻⁶ have argued for a higher SCC on various grounds. A key potential
27 contributor to increasing the SCC is the possibility that ongoing climate change will cause
28 elements of the climate system to pass ‘tipping points’ leading to irreversible damages^{7,8}.

29 Existing scientific studies suggest there are multiple climate tipping points that could be
30 triggered this century or next if climate change continues unabated^{7,8}, and there are causal
31 interactions between tipping events such that tipping one element affects the likelihoods of
32 tipping others⁸ (Fig. 1). The likelihood of specific tipping events varies, but is generally
33 expected to increase with global temperature^{7,8}. However, internal variability within the
34 climate system, and relatively rapid anthropogenic forcing, mean that even if deterministic
35 tipping points could be precisely identified, the actual systems could be tipped earlier or
36 later⁹. Thus, any assessment of their policy implications needs to represent the stochastic
37 uncertainty surrounding when tipping points could occur¹⁰. Furthermore, the impacts of
38 passing different tipping points are expected to vary^{7,11}, and to unfold at different rates
39 depending on the internal timescale of the part of the climate system being tipped^{7,11}.

40 Relative to this scientific understanding, most cost-benefit analyses of climate change only
41 allow for simple and scientifically unrealistic representations of climate tipping points¹¹.
42 Most previous IAM studies of climate catastrophes have treated them in a deterministic
43 fashion, sometimes giving them a probability distribution^{5,12-15}. Some recent IAM studies
44 have considered one stochastic climate tipping point impacting economic output¹⁰, non-
45 market welfare¹⁶, climate sensitivity¹⁷, or carbon cycle feedbacks¹⁷. This can lead to up to
46 200% increases in the SCC in extreme cases¹⁰, with the results clearly sensitive to the

47 timescale over which tipping point impacts unfold, as well as the final magnitude of those
48 impacts¹⁰. However, there has been little consideration of multiple tipping points and
49 interactions between them, or of how an appropriate representation of risk aversion affects
50 the optimal response to the prospect of future tipping points.

51 A recent IAM study¹⁸ has examined three loosely-defined tipping points that instantaneously
52 alter climate sensitivity, carbon cycle feedbacks, or economic output, and interact via their
53 effects on atmospheric CO₂, global temperature, or economic output. Here we consider five
54 carefully-defined tipping points^{7,8} and the direct causal interactions between them identified
55 by scientific experts⁸ (Fig. 1). These interactions occur primarily via aspects of the climate
56 system that are not resolved in simple IAMs. The impacts of our tipping points unfold at a
57 rate appropriate for the system being tipped, in contrast with instantaneous changes^{17,18} in
58 climate sensitivity and carbon cycle feedbacks which are scientifically questionable¹⁰. Our
59 tipping points principally affect economic output, although we also consider their feedback
60 effects on the carbon cycle. Instead of arbitrarily specifying the likelihood of the tipping
61 points¹⁸ we calibrate their likelihoods (and the causal interactions between them) based on the
62 results of an existing expert elicitation⁸. Furthermore, in contrast to recent work¹⁸, we alter
63 the specification of the social planner's preferences regarding risk aversion and
64 intergenerational equity, in a manner appropriate for the stochastic uncertainty surrounding
65 future tipping points.

66

67 **Modelling tipping points**

68 We use the dynamic stochastic integration of climate and economy (DSICE) framework¹⁹ to
69 incorporate five stochastic tipping points and causal interactions between them into the 2013
70 version of the well-known DICE model²⁰ (see Methods, Supplementary Figs. 1,2). This

71 means solving a 16-dimensional stochastic model – the first time in the field of economics of
72 climate change that an analysis on such a scale has been accomplished (our previous work¹⁰
73 solved a 7-dimensional system, whereas other simplified stochastic versions¹⁷ of DICE only
74 consider 4 dimensions). In our stochastic version of the DICE model, we use annual time
75 steps, and calibrate parameters in the carbon cycle and temperature modules against the
76 emulated median response of complex climate models for the four RCP (representative
77 concentration pathway) scenarios²¹ (see Supplementary Methods). In a deterministic setting
78 within our model (without considering climate tipping points) our calibration gives a social
79 cost of carbon in 2010 of \$15/tCO₂ (all results are in 2010 US dollars). For reference,
80 Nordhaus' DICE-2013R model²⁰ which uses five-year time steps and is calibrated against one
81 RCP scenario also has a 2010 SCC of \$15/tCO₂.

82 In IAMs such as DICE, greater emission control at present mitigates damages from climate
83 change in the future but limits consumption and/or capital investment today. A 'social
84 planner' is assumed to weigh these costs and benefits of emission control to maximize the
85 expected present value of global social welfare. When faced with stochastic uncertainty about
86 future tipping events, the social planner's response will depend on their preferences regarding
87 risk and smoothing consumption. DICE adopts a specification of risk aversion that is
88 inversely tied to the decision maker's preferences to smooth consumption over time (i.e. the
89 inter-temporal elasticity of substitution). Thus, a high inter-temporal elasticity of substitution
90 is taken to imply a low risk aversion. In the baseline DICE model, risk aversion $RA=1.45$,
91 and inter-temporal elasticity of substitution $IES=1/1.45$. However, empirical economic data
92 do not support this inverse proportionality (implying time separable utility) and suggest
93 instead decoupling these preferences²². Hence we incorporated 'Epstein-Zin' (EZ)
94 preferences²² using default parameter settings²³ of $RA=3.066$ and $IES=1.5$, which are
95 consistent with empirical findings²³ (implying time non-separable utility). Estimates of $IES>1$

96 have been obtained from e.g. stockholder data²⁴, IES=1.5 is used in a long-run risk model^{19,25},
97 and the upper bound is considered²³ to be IES ~2. Using IES=1.5, equity returns data²³
98 suggest RA=3.066, which is in the range RA=3-4 from a separate study of equity premiums
99 of rare disasters²⁶, with the upper bound considered²⁵ to be RA~10.

100 The five interacting, stochastic, potential climate tipping points^{7,8} (Fig. 1, Table 1) represent
101 reorganisation of the Atlantic Meridional Overturning Circulation (AMOC), disintegration of
102 the Greenland Ice Sheet (GIS), collapse of the West Antarctic Ice Sheet (WAIS), dieback of
103 the Amazon rainforest (AMAZ), and shift to a more persistent El-Niño regime (ENSO). We
104 used published expert elicitation results⁸ to derive the likelihoods (see Methods) of each of
105 the five tipping events (Table 1), and the causal interactions between them (Fig. 1,
106 Supplementary Table 1). By causal interaction we mean that the hazard rate of each tipping
107 point depends on the state of the others.

108 For each tipping event we specified a transition timescale¹⁰ (Table 1, see Methods) – i.e. how
109 long it would take for the full impacts to unfold, based on current scientific understanding of
110 the timescales of the systems being tipped^{7,11} (e.g. ice sheets melt more slowly than the ocean
111 circulation can reorganise). Recognising the scientific uncertainty surrounding transition
112 times we explore a factor of 5 uncertainty range in either direction. We must also specify a
113 final damage for each tipping event (Table 1, see Methods), taken to be an irreversible
114 percentage reduction in world GDP. This is the most problematic and debatable part of the
115 parameterisation, because of a gross shortage of scientific and economic estimates of tipping
116 point damages¹¹. We can make some scientific inferences about relative damages (e.g. based
117 on the eventual contributions of different ice sheets to sea-level rise). Past studies with DICE
118 have loosely associated a 25-30% reduction in GDP comparable with the Great Depression
119 with a collapse of the AMOC^{27,28}, but when combined with other tipping points this could
120 lead to excessively high overall damages. Our assigned damages for individual tipping points

121 range from 5-15% reduction in GDP with a combined reduction in GDP if all five tipping
122 events occur and complete their transitions of 38%. However, due to relatively low
123 probabilities and long transition timescales, the expected tipping point damages in our default
124 scenario only amount to 0.53% of GDP in 2100 and 1.89% of GDP in 2200. In our sensitivity
125 analysis we consider a factor of 2-3 total uncertainty range in final damages for each tipping
126 point. Finally, we include some conservative effects of tipping particular systems on the
127 carbon cycle (Table 1, see Methods).

128

129 **Optimal policy**

130 The result of including multiple interacting tipping points under EZ preferences (Fig. 2) is a
131 nearly 8-fold increase in the initial social cost of carbon from \$15/tCO₂ in the baseline model
132 (grey line) to \$116/tCO₂ (black line). Across 10,000 sample paths of the model there are
133 cases where one or more tipping points still occur, leading to uncertainty ranges for the key
134 variables (grey shaded areas). The emissions control rate jumps from ~18% to ~56% in 2010
135 and rises to 100% by 2050, effectively shutting down fossil fuel CO₂ emissions – whereas in
136 the baseline model emissions continue into the next the century. The average atmospheric
137 carbon peaks in the 2030s at 415 ppm and then declines (due to ongoing ocean carbon
138 uptake) – whereas in the baseline model atmospheric CO₂ continues to rise to ~650 ppm by
139 2100. Temperature rise slows down and is almost stable around 1.4 °C above pre-industrial
140 by 2100 – whereas in the baseline model warming continues and approaches 3 °C by 2100.
141 Following the expected path (black line) there is only an 11% probability of one or more
142 tipping events by 2100, reduced from 46% in the baseline model, or 87% under a prescribed
143 RCP8.5 emissions scenario (Table 2).

144 A factor of 2.4 increase from the baseline SCC to \$36/tCO₂ is just due to the change to EZ
145 preferences (dashed black line, Fig. 2), with a further factor of 3.2 increase due to the
146 potential for multiple tipping points. With just EZ preferences (and no stochastic tipping
147 points) the initial emissions control rate increases from ~18% to ~29% with 100% emissions
148 control in 2100. Atmospheric carbon peaks around 550 ppm, with surface temperature
149 stabilising around 2.3 °C above pre-industrial.

150

151 **Tipping point interactions**

152 In the full model, there are both positive and negative causal interactions between tipping
153 points (Fig. 1, Supplementary Table 1), which are conservatively calibrated (see Methods).
154 Hence their inclusion has only a modest net effect on the expected SCC, increasing it from
155 \$109/tCO₂ to \$116/tCO₂ (see also Supplementary Fig. 3). However, a specific sample path
156 where multiple tipping events occur before 2200 (Fig. 3, solid line) reveals that some tipping
157 point interactions can have a strong effect on the time evolution of the SCC. Considering a no
158 interactions sample path (Fig. 3, dashed line) shows that in general, passing a tipping point
159 reduces the incentive to mitigate and therefore lowers the SCC, because it can no longer be
160 avoided. However, with interactions, tipping of the GIS significantly increases the likelihood
161 of AMOC tipping (which is assumed to be the most damaging event) hence this causes a
162 large increase in the SCC in order to try to avoid AMOC tipping. (This is consistent with
163 previous suggestions^{29,30} that tipping points can create multiple optima – here for the SCC
164 and corresponding emissions³⁰.) Subsequent tipping of AMOC greatly reduces the SCC.
165 Tipping of ENSO causes a small increase in the SCC because it increases the likelihood of
166 tipping the Amazon. Subsequent tipping of the Amazon halves the SCC because there is now
167 an unavoidable extra source of carbon to the atmosphere and only WAIS left to tip. There are

168 other sample paths where the first tipping event does not increase the likelihood of others so
169 the SCC drops – e.g. when the Amazon rainforest tips first (Supplementary Fig. 4).

170 The social cost of carbon therefore depends on whether tipping events occur and in which
171 order. This can also be seen by looking at the sample paths for the earliest and sole tipping
172 before 2100 of each element (Supplementary Fig. 5). If the GIS tips first this leads to the
173 highest SCC path and the most stringent emission control, reaching 100% before 2040,
174 because of the increased risk of AMOC collapse. If the AMOC tips first, this gives the lowest
175 SCC path because it has the greatest damages, which can no longer be avoided – yet emission
176 control remains above 60% and the SCC remains above \$110/tCO₂. If the Amazon tips first,
177 this also lowers SCC and emission control, but it leads to the highest atmospheric carbon and
178 temperature trajectory because of an accompanying carbon source. If ENSO tips first, this
179 slightly increases emission control because the likelihood of the AMAZ tipping is increased.
180 If the WAIS tips first, there is little effect on emission control because it only slightly
181 increases the likelihood of tipping the AMOC and GIS. CO₂ emissions trajectories
182 (Supplementary Fig. 6) therefore depend on the contemporaneous state of tipping elements.

183

184 **Sensitivity analysis**

185 The high social cost of carbon is robust to sensitivity analyses (see Methods). Combined
186 variations in assumed transition times and final damages of the tipping points give a full
187 range in initial SCC of \$50-166/tCO₂ (Supplementary Table 2). With pessimistic settings for
188 the expert assessment of interactions between tipping elements (Supplementary Table 3), the
189 SCC increases from \$116/tCO₂ to \$121/tCO₂. Including an endogenous transition time for the
190 GIS gives only a slight reduction in SCC to \$114/tCO₂ because its damages tend to be

191 discounted away anyway. Allowing all tipping elements to have an endogenous transition
192 time reduces SCC to \$94/tCO₂.

193 Retaining an intertemporal elasticity of substitution IES=1.5 but increasing risk aversion to
194 RA=10 increases the SCC from \$116/tCO₂ to \$146/tCO₂. With the original RA=3.066 and an
195 upper limit of IES=2 the SCC increases to \$151/tCO₂. Using the default DICE settings of
196 IES=1/1.45 and RA=1.45 gives an SCC of \$28/tCO₂, a factor 1.9 increase from the default
197 \$15/tCO₂ due to the five interacting tipping points. Thus, EZ preferences magnify the effect
198 of including potential future tipping points, causing a factor 3.2 (rather than 1.9) increase in
199 the SCC. To disentangle the effect of IES and RA, we also investigate a case with IES=1.5
200 and RA=1/1.5, which gives an SCC of \$104/tCO₂. That is, when we incorporate the climate
201 tipping risks, using time separable preferences as in DICE, an increase from IES=1/1.45 (and
202 RA=1.45) to IES=1.5 (and RA=1/1.5) leads to a factor 3.7 increase in the SCC, and the
203 additional change to our default time non-separable EZ preferences (IES=1.5, RA=3.066)
204 leads to an extra SCC of \$12/tCO₂.

205

206 **Discussion and conclusion**

207 Putting our results in scientific context, there is already evidence that major ice sheets are
208 losing mass at an accelerating rate^{31,32}. GIS mass loss is estimated to be contributing ~0.7
209 mm/yr to sea-level rise³³, with a corresponding increase in freshwater flux to the North
210 Atlantic³⁴ since 1990 of ~0.01 Sv. Although modest at present, this and other contributors to
211 increasing freshwater input to the North Atlantic³⁵, are thought⁸ to increase the likelihood of
212 AMOC tipping, and our results suggest this should be increasing the incentive to control CO₂
213 emissions. WAIS mass loss is contributing ~0.35 mm/yr to sea-level rise³², and there is
214 evidence that parts of the West Antarctic ice sheet are already in irreversible retreat³⁶⁻³⁸. If the

215 WAIS has already passed a tipping point then mitigation cannot avoid it, but our results
216 suggest this should not significantly reduce the incentive to mitigate to try to avoid other
217 tipping events.

218 Our results and policy recommendations differ considerably from another recent study
219 considering multiple tipping points¹⁸, which recommends at most a doubling of the social
220 cost of carbon (SCC) that allows CO₂ emissions to continue to grow past mid-century, with
221 temperature ultimately peaking at just under 3 °C. In contrast, our results recommend a
222 nearly 8-fold increase in the SCC to drive a cessation of CO₂ emissions by mid-century,
223 which limits warming to <1.5 °C. This very different outcome is a result of our different
224 specification of tipping points together with our change in decision maker preferences to
225 something more appropriate for such stochastic climate risks.

226 There are several caveats with the DICE modelling approach used here (and the simplified
227 version of DICE used elsewhere¹⁸). In the climate component of the model, the ocean carbon
228 sink is too strong³⁹, causing it to overestimate the effect of emissions reductions on
229 atmospheric CO₂ and temperature, especially beyond 2100. We only consider one value for
230 equilibrium climate sensitivity (2.9 °C following DICE-2013), whereas the IPCC likely
231 range⁴⁰ spans 1.5-4.5 °C. Nevertheless, the DICE prediction that a shut-down of CO₂
232 emissions by mid-century will lead to ~1.5 °C warming, is compatible with more detailed
233 probabilistic projections^{41,42} varying climate sensitivity (noting that DICE shuts down
234 emission faster but then does not allow for net carbon dioxide removal in the second half of
235 this century^{41,42}).

236 The economic component of DICE allows for an unrealistic instantaneous adjustment of
237 emissions (to e.g. a control rate >0.5), whereas in reality emissions control rates are low and
238 there are lags in ramping them up, for example due to the lifetime of coal-fired power

239 stations. However, recent energy-economic model studies^{41,42} show that it is technologically
240 feasible to increase the emissions control rate to 100%, and thus achieve net zero CO₂
241 emissions, by mid-century. The assumed costs of mitigation options in DICE are also
242 relatively low⁴³, whereas energy-economic models⁴¹ indicate that limiting warming to 1.5 °C
243 would be considerably more expensive than limiting it to 2 °C, especially between now and
244 2030. Despite these uncertainties, in a real options analysis framework⁴⁴, paying up front now
245 to minimise the future risk of climate tipping points can still be the logical and cost-effective
246 option for societies. Furthermore, acknowledging that society also faces other potential
247 tipping points (e.g. disease pandemics) should increase the willingness to pay to avert any
248 one of them⁴⁵, even though we should not necessarily avert all of them⁴⁵. The decision to try
249 to avert climate tipping points depends crucially on a relatively high risk aversion⁴⁵,
250 consistent with our findings.

251 In summary, our results illustrate that the prospect of multiple interacting climate tipping
252 points with irreversible economic damages ought to be provoking very strong mitigation
253 action, on the part of ‘social planners’ – including governments signed up to the United
254 Nations Framework Convention on Climate Change. Under realistic preferences under
255 uncertainty, the optimal policy involves a shutdown of carbon emissions by mid-century.

256

257 **References**

- 258 1 Interagency Working Group on Social Cost of Carbon, Social Cost of Carbon for
259 Regulatory Impact Analysis - Under Executive Order 12866. United States
260 Government, 2010.
- 261 2 Interagency Working Group on Social Cost of Carbon, Technical Update of the Social
262 Cost of Carbon for Regulatory Impact Analysis. United States Government, 2013.

263 3 Dietz, S., High impact, low probability? An empirical analysis of risk in the
264 economics of climate change. *Climatic Change* 108, 519-541 (2011).

265 4 Kopp, R.E., Golub, A., Keohane, N.O., & Onda, C., The Influence of the
266 Specification of Climate Change Damages on the Social Cost of Carbon. *Economics:
267 The Open-Access, Open-Assessment E-Journal* 6 (2012-13), 1-40 (2012).

268 5 Ackerman, F. & Stanton, E.A., Climate Risks and Carbon Prices: Revising the Social
269 Cost of Carbon *Economics: The Open-Access, Open Assessment E-Journal* 6 (2012-
270 10), 1-25 (2012).

271 6 van den Bergh, J.C.J.M. & Botzen, W.J.W., A lower bound to the social cost of CO2
272 emissions. *Nature Clim. Change* 4 (4), 253-258 (2014).

273 7 Lenton, T.M. *et al.*, Tipping Elements in the Earth's Climate System. *Proceedings of
274 the National Academy of Sciences* 105 (6), 1786-1793 (2008).

275 8 Kriegler, E., Hall, J.W., Held, H., Dawson, R., & Schellnhuber, H.J., Imprecise
276 probability assessment of tipping points in the climate system. *PNAS* 106 (13), 5041-
277 5046 (2009).

278 9 Lenton, T.M., Early warning of climate tipping points. *Nature Climate Change* 1,
279 201-209 (2011).

280 10 Lontzek, T.S., Cai, Y., Judd, K.L., & Lenton, T.M., Stochastic integrated assessment
281 of climate tipping points indicates the need for strict climate policy. *Nature Climate
282 Change* 5 (4), 441-444 (2015).

283 11 Lenton, T.M. & Ciscar, J.-C., Integrating tipping points into climate impact
284 assessments. *Climatic Change* 117 (3), 585-597 (2013).

285 12 Mastrandrea, M.D. & Schneider, S.H., Probabilistic Integrated Assessment of
286 "Dangerous" Climate Change. *Science* 304 (5670), 571-575 (2004).

- 287 13 Kosugi, T., Integrated Assessment for Setting Greenhouse Gas Emission Targets
288 under the Condition of Great Uncertainty about the Probability and Impact of Abrupt
289 Climate Change. *Journal of Environmental Informatics* 14 (2), 89-99 (2009).
- 290 14 Ackerman, F., Stanton, E.A., & Bueno, R., Fat tails, exponents, extreme uncertainty:
291 Simulating catastrophe in DICE. *Ecological Economics* 69 (8), 1657-1665 (2010).
- 292 15 Weitzman, M.L., GHG Targets as Insurance Against Catastrophic Climate Damages.
293 *Journal of Public Economic Theory* 14 (2), 221-244 (2012).
- 294 16 Cai, Y., Judd, K.L., Lenton, T.M., Lontzek, T.S., & Narita, D., Environmental tipping
295 points significantly affect the cost-benefit assessment of climate policies.
296 *Proceedings of the National Academy of Sciences* 112 (15), 4606-4611 (2015).
- 297 17 Lemoine, D. & Traeger, C., Watch Your Step: Optimal Policy in a Tipping Climate.
298 *American Economic Journal: Economic Policy* 6 (1), 137-166 (2014).
- 299 18 Lemoine, D. & Traeger, C.P., The Economics of Tipping the Climate Dominoes.
300 *Nature Climate Change* (in press).
- 301 19 Cai, Y., Judd, K.L., & Lontzek, T.S., The Social Cost of Carbon with Economic and
302 Climate Risks. <http://arxiv.org/abs/1504.06909> (2015).
- 303 20 Nordhaus, W., Estimates of the Social Cost of Carbon: Concepts and Results from the
304 DICE-2013R Model and Alternative Approaches. *Journal of the Association of*
305 *Environmental and Resource Economists* 1 (1), 273-312 (2014).
- 306 21 Meinshausen, M. et al., The RCP greenhouse gas concentrations and their extensions
307 from 1765 to 2300. *Climatic Change* 109, 213-241 (2011).
- 308 22 Epstein, L.G. & Zin, S.E., Substitution, risk aversion, and the temporal behavior of
309 consumption and asset returns: a theoretical framework. *Econometrica* 57 (4), 937-
310 969 (1989).

- 311 23 Pindyck, R.S. & Wang, N., The Economic and Policy Consequences of Catastrophes.
312 *American Economic Journal: Economic Policy* 5 (4), 306-339 (2013).
- 313 24 Vissing-Jørgensen, A. & Attanasio, O.P., Stock-Market Participation, Intertemporal
314 Substitution, and Risk-Aversion. *American Economic Review* 93 (2), 383-391 (2003).
- 315 25 Bansal, R. & Yaron, A., Risks for the Long Run: A Potential Resolution of Asset
316 Pricing Puzzles. *The Journal of Finance* 59 (4), 1481-1509 (2004).
- 317 26 Barro, R.J., Rare Disasters, Asset Prices, and Welfare Costs. *American Economic*
318 *Review* 99 (1), 243-264 (2009).
- 319 27 Nordhaus, W.D., Expert Opinion on Climatic Change. *American Scientist* 82, 45-51
320 (1994).
- 321 28 Nordhaus, W.D. & Boyer, J., *Warming the World. Models of Global Warming*. (MIT
322 Press, Cambridge, Massachusetts, USA, 2000).
- 323 29 Baumol, W.J., On Taxation and the Control of Externalities. *The American Economic*
324 *Review* 62 (3), 307-322 (1972).
- 325 30 Kopp, R.E. & Mignone, B.K., The U.S. Government's Social Cost of Carbon
326 Estimates after Their First Two Years: Pathways for Improvement. *Economics: The*
327 *Open-Access, Open-Assessment E-Journal* 6 (2012-15), 1-41 (2012).
- 328 31 Khan, S.A. *et al.*, Sustained mass loss of the northeast Greenland ice sheet triggered
329 by regional warming. *Nature Clim. Change* 4 (4), 292-299 (2014).
- 330 32 Harig, C. & Simons, F.J., Accelerated West Antarctic ice mass loss continues to
331 outpace East Antarctic gains. *Earth and Planetary Science Letters* 415 (0), 134-141
332 (2015).
- 333 33 Csatho, B.M. *et al.*, Laser altimetry reveals complex pattern of Greenland Ice Sheet
334 dynamics. *Proceedings of the National Academy of Sciences* 111 (52), 18478-18483
335 (2014).

336 34 Bamber, J., van den Broeke, M., Ettema, J., Lenaerts, J., & Rignot, E., Recent large
337 increases in freshwater fluxes from Greenland into the North Atlantic. *Geophysical*
338 *Research Letters* 39 (19), L19501 (2012).

339 35 Peterson, B.J. *et al.*, Increasing river discharge to the Arctic Ocean. *Science* 298,
340 2171-2173 (2002).

341 36 Joughin, I., Smith, B.E., & Medley, B., Marine Ice Sheet Collapse Potentially Under
342 Way for the Thwaites Glacier Basin, West Antarctica. *Science* 344 (6185), 735-738
343 (2014).

344 37 Rignot, E., Mouginot, J., Morlighem, M., Seroussi, H., & Scheuchl, B., Widespread,
345 rapid grounding line retreat of Pine Island, Thwaites, Smith, and Kohler glaciers,
346 West Antarctica, from 1992 to 2011. *Geophysical Research Letters* 41 (10), 3502-
347 3509 (2014).

348 38 Wouters, B. *et al.*, Dynamic thinning of glaciers on the Southern Antarctic Peninsula.
349 *Science* 348 (6237), 899-903 (2015).

350 39 Glotter, M.J., Pierrehumbert, R.T., Elliott, J.W., Matteson, N.J., & Moyer, E.J., A
351 simple carbon cycle representation for economic and policy analyses. *Climatic*
352 *Change* 126 (3-4), 319-335 (2014).

353 40 Bindoff, N.L. *et al.*, Detection and Attribution of Climate Change: from Global to
354 Regional in *Climate Change 2013: The Physical Science Basis. Contribution of*
355 *Working Group I to the Fifth Assessment Report of the Intergovernmental Panel on*
356 *Climate Change*, edited by T.F. Stocker, D. Qin, G.-K. Plattner, M. Tignor, S.K.
357 Allen, J. Boschung, A. Nauels, Y. Xia, V. Bex and P.M. Midgley (Cambridge
358 University Press, Cambridge, United Kingdom and New York, NY, USA, 2013).

359 41 Rogelj, J. *et al.*, Energy system transformations for limiting end-of-century warming
360 to below 1.5 [deg]C. *Nature Clim. Change* 5 (6), 519-527 (2015).

361 42 Rogelj, J. *et al.*, Zero emission targets as long-term global goals for climate
362 protection. *Environmental Research Letters* 10 (10), 105007 (2015).

363 43 Nordhaus, W., *The Climate Casino: Risk, Uncertainty, and Economics for a Warming*
364 *World*. (Yale University Press, 2013).

365 44 Anda, J., Golub, A., & Strukova, E., Economics of climate change under uncertainty:
366 Benefits of flexibility. *Energy Policy* 37 (4), 1345-1355 (2009).

367 45 Martin, I.W.R. & Pindyck, R.S., Averting Catastrophes: The Strange Economics of
368 Scylla and Charybdis. *American Economic Review* 105 (10), 2947-2985 (2015).

369

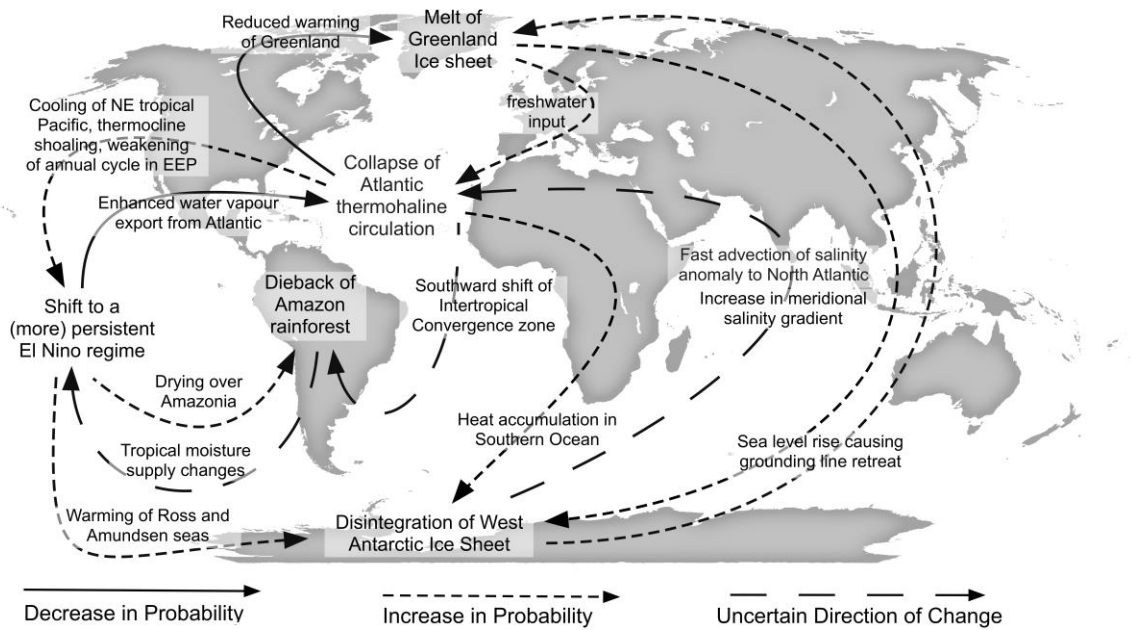
370 Correspondence and requests for materials should be addressed to t.m.lenton@exeter.ac.uk or
371 lontzek@gmail.com

372 **Acknowledgments.** We thank Kenneth L. Judd and participants of the 2015 Annual
373 Conference of the European Association of Environmental and Resource Economics for
374 comments. Y.C. was supported by NSF (SES-0951576 and SES-1463644). T.S.L. was
375 supported by the Züricher Universitätsverein, the University of Zurich, and the Ecosciencia
376 Foundation. T.M.L. was supported by a Royal Society Wolfson Research Merit Award and
377 the European Commission HELIX project (ENV.2013.6.1-3). Supercomputer support was
378 provided by Blue Waters (NSF awards OCI-0725070 and ACI-1238993, and the state of
379 Illinois).

380 **Author contributions.** Y.C., T.M.L. and T.S.L. designed research, performed research, and
381 wrote the paper.

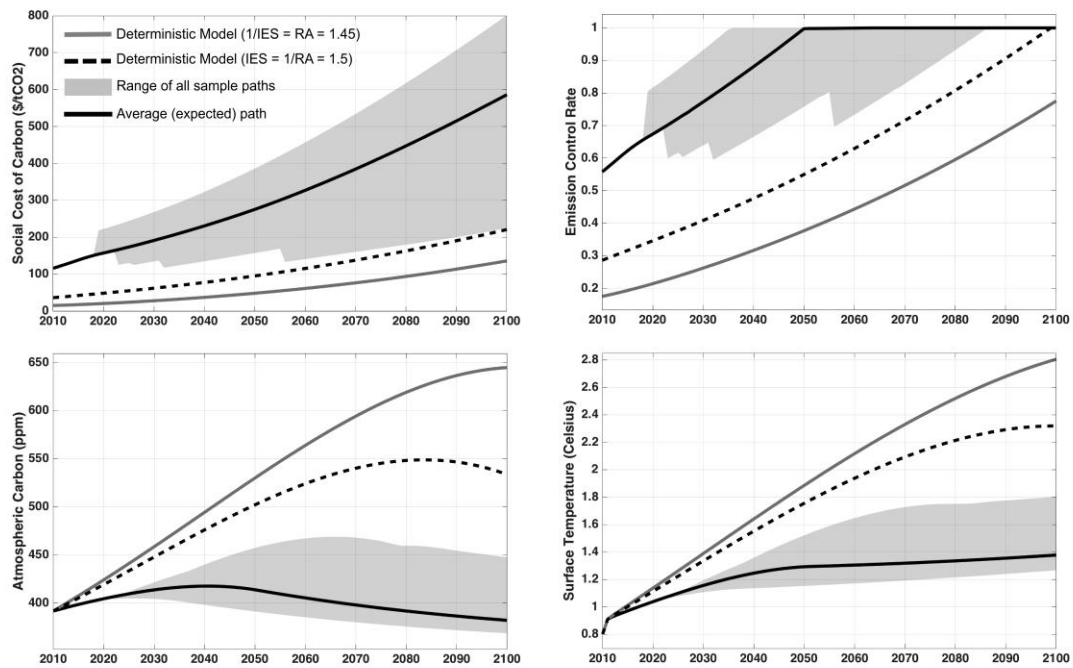
382

383 **Figure legends**



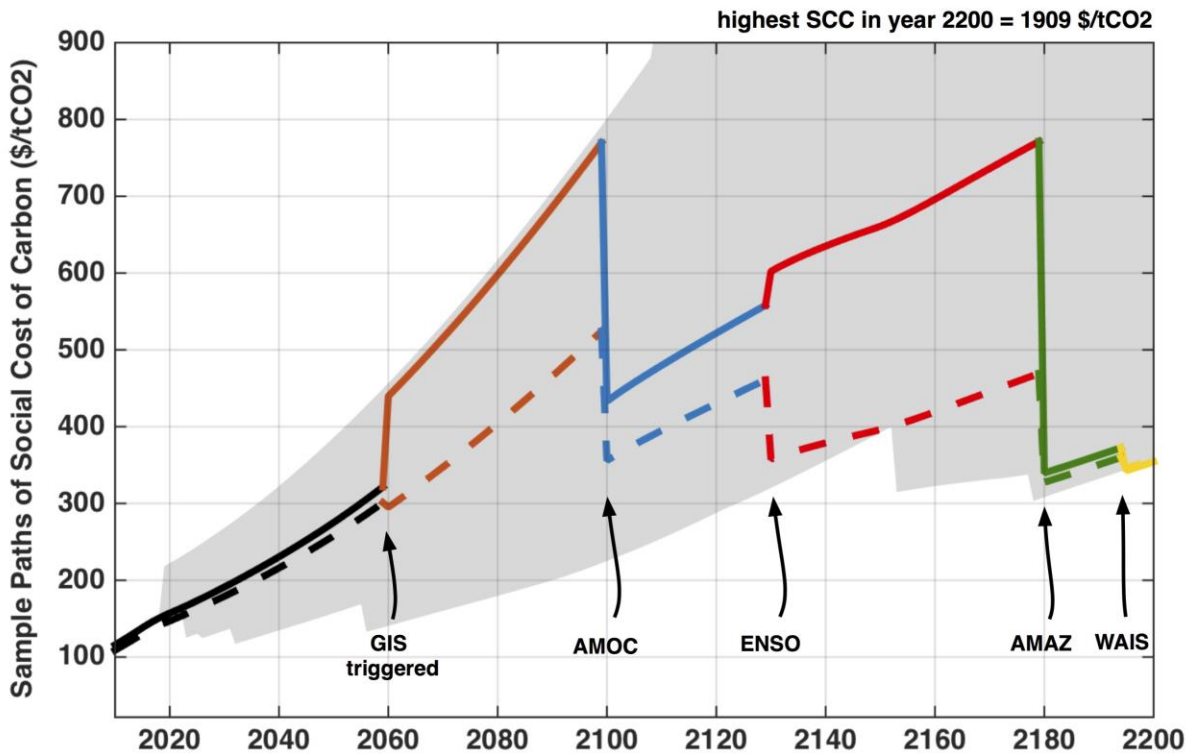
384

385 **Figure 1.** Map of the five climate tipping events considered here and the causal interactions
 386 between them previously identified in an expert elicitation⁸.



387

388 **Figure 2.** Results for: (a) the social cost of carbon, (b) emissions control policy, (c)
 389 atmospheric carbon (ppm), and (d) surface temperature change (above pre-industrial), in the
 390 baseline deterministic model (grey), the deterministic model with Epstein-Zin preferences
 391 (dashed black), and the expected path of stochastic model with multiple interacting tipping
 392 points (black). The grey-shaded area shows the range of sample paths from 10,000
 393 simulations of the stochastic model (see Supplementary Figure 3 for the analogous case
 394 without interaction).



395

396 **Figure 3.** Example sample paths of the social cost of carbon (SCC) in $\$/tCO_2$ with multiple
 397 tipping points interacting (solid line) and not interacting (dashed line) to highlight the effect
 398 of causal interactions between tipping events.

399

400 **Tables**

401

402 **Table 1.** Hazard rate, transition time, final damages and carbon cycle effect for each tipping
 403 element, with uncertainty ranges (in parentheses) considered in the sensitivity analysis.

Tipping element	Hazard rate (%/yr/K)	Transition time (years)	Final damages (% GDP)	Carbon cycle effect
AMOC	0.063	50 (10-250)	15 (10-20)	No effect
GIS	0.188	1500 (300-7500)	10 (5-15)	100 GtC over transition
WAIS	0.104	500 (100-2500)	5 (2.5-7.5)	100 GtC over transition
AMAZ	0.163	50 (10-250)	5 (2.5-7.5)	50 GtC over transition
ENSO	0.053	50 (10-250)	10 (5-15)	0.2 GtC/yr permanent

404

405

406

407 **Table 2.** Expected tipping point probabilities (%) by years 2100 and 2200, based on 10,000
 408 model runs of the DSICE model¹⁹ with five stochastic tipping points, and those that would be
 409 obtained from the temperature paths in the deterministic baseline model without tipping
 410 points, or under prescribed RCP 8.5 emissions.

Number of tipping events	Stochastic tipping points (interacting)		Stochastic tipping points (no interaction)		Baseline model temperature path*		RCP8.5 temperature path**	
	2100	2200	2100	2200	2100	2200	2100	2200
1	10.8	24.38	12.04	26.88	34.28	23.03	29.69	0
2	0.65	4.14	0.72	4.08	10.03	31.31	30.73	0
3	0.04	0.42	0.05	0.41	1.81	24.7	19.08	0.33
4	0	0.02	0	0.02	0.18	10.1	6.76	16.87
5	0	0.01	0	0	0	2.29	0.85	82.80
Cumulative probability	11.49	28.97	12.81	31.39	46.30	91.43	87.11	100

411 *2.8 °C warming in 2100, 2.76 °C in 2200

412 **4.7 °C warming in 2100, 7.5 °C in 2200

413

414

415 **Methods**

416 **Summary**

417 We use the DSICE model^{10,19} (Supplementary Fig. 1) to compute the socially optimal
418 reduction of global greenhouse gas emissions under the possibility of five interacting climate
419 tipping points. The baseline deterministic model without tipping points is based on the 2013
420 version of DICE²⁰, but uses parameters in the carbon cycle and temperature system calibrated
421 against all four RCP scenarios (see Supplementary Methods), and solves on an annual time
422 step. DICE comprises one state variable for the capital stock, representing the world
423 economy, a three-box carbon cycle module, and a two-box climate. To this we add a 10-
424 dimensional system of interacting tipping elements.

425 For each of five tipping elements we have a discrete binary state indicating whether its
426 corresponding tipping process has been already triggered or not, and a continuous state
427 variable indicating the contemporaneous length of the transition process. The occurrence of
428 each climate tipping point is modeled by a Markov process and its timing is not known at the
429 times of decisions. The endogenous hazard rate (/yr/K) for each tipping event is assumed zero
430 up to 1 °C warming above pre-industrial levels (reached in about 2015 in the model) and
431 increases linearly with global warming above 1 °C at a rate derived from published expert
432 elicitation results⁸. The conditional probabilities representing changes to the other hazard
433 rates should a particular system tip are conservatively specified given wide ranges in the
434 expert assessment⁸. The transition timescale¹⁰ of each tipping element is based on current
435 scientific understanding of the timescales at which specific climate subsystems can transition
436 into an alternative state, with a factor of 5 uncertainty range in either direction considered in
437 the sensitivity analysis. Tipping points are assumed to directly impact economic output and
438 their relative final damages are based on scientific understanding. The absolute final damages

439 of individual tipping events are highly uncertain and are varied in the sensitivity analysis over
440 a factor of 2-3 range, giving a range in total reduction in GDP if all five tipping events occur
441 of 23%-50%. In addition to the impacts of tipping points on economic output we also include
442 conservative effects of tipping particular systems on the carbon cycle, implemented as
443 exogenous emissions to the atmosphere. The stochastic model is solved using a
444 supercomputer^{19,46}, to generate 10,000 stochastic sample paths, with the expected path
445 calculated as the average of all paths.

446 In the following, we detail the specific modifications to the DICE-2013R model and refer to
447 Nordhaus⁴³ for calibration and formulations of the remaining parts of the model.

448

449 **Calibration of tipping elements and interactions between them**

450 As in previous work¹⁰ we define three phases to the tipping process for each tipping element
451 (Supplementary Fig. 2). In the first, pre-trigger phase, the additional damage from a tipping
452 point is 0. In the second, transition phase, there is a positive, but not stationary additional
453 damage level. In the third and final, post-tipping phase the tipping element is in a new,
454 absorbing state, with a constant (irreversible) damage level.

455 For each tipping element, i , after a tipping point is passed, a persistent climate impact state,
456 the additional damage factor $J_{i,t}$ will increase continuously from a minimal level (i.e., $J_{i,t} =$
457 0) to some maximum level ($\bar{J}_i > 0$), implying that $J_{i,t+1} = \min\{J_{i,t} + \Delta_{i,t}, \bar{J}_i\}I_{i,t}$, where $\Delta_{i,t}$ is
458 the incremental impact level from stage t to $t + 1$ of tipping element i . In our default case,
459 $\Delta_{i,t}$ denotes linear increments, but these increments become nonlinear in the sensitivity case
460 with endogenous transition time. We use $I_{i,t}$ as the indicator function to denote for each
461 tipping element i the pre-trigger state of the world as $I_{i,t} = 0$ and the post-trigger state of the

462 world as $I_{i,t} = 1$, where $I_{i,t}$ is a jump process with a Markovian hazard rate. The latter is
 463 endogenous with respect to the contemporaneous level of global average atmospheric
 464 temperature, T_t^{AT} . Furthermore, to model causal relationships between the tipping elements
 465 the Markovian hazard rate for tipping element i also depends on whether a tipping process of
 466 climate tipping element j has been triggered. We do not explicitly consider other indicators
 467 for tipping, e.g., the gradient of temperature⁴⁷. The transition function for $I_{i,t}$ from stage t to
 468 stage $t + 1$ is $I_{i,t+1} = g_i^I(\mathbf{I}_t, T_t^{AT}, \omega_{i,t}^I)$, where \mathbf{I}_t is the vector of the indicator functions for
 469 the five climate tipping elements $(I_{1,t}, \dots, I_{5,t})$ and $\omega_{i,t}^I$ is a random process. With $J_{i,t+1} =$
 470 $\min\{J_{i,t} + \Delta_{i,t}, \bar{J}_i\}$ the impact factor on the economy becomes

$$471 \quad \Omega_t(T_t^{AT}, \mathbf{J}_t, \mathbf{I}_t) = \frac{\prod_i (1 - I_{i,t} J_{i,t})}{1 + \pi_2 (T_t^{AT})^2} \quad (1)$$

472 where T_t^{AT} is the average global atmospheric temperature and π_2 is a coefficient in the
 473 damage function. (The impact of global warming on the economy is reflected by a convex
 474 damage function of atmospheric temperature, which is a standard feature of the DICE model
 475 – a deterministic model specification would simply be to fix all $I_{i,t}$ at 0.) We specify the
 476 probability transition matrix of the tipping process i at time t as

$$477 \quad \begin{bmatrix} 1 - p_{i,t} & p_{i,t} \\ 0 & 1 \end{bmatrix} \quad (2)$$

478 where its (n, m) element is the transition probability from state n to m for $I_{i,t}$, and $p_{i,t} = 1 -$
 479 $\exp(-B_i(\mathbf{I}) \max\{0, T_t^{AT} - 1\})$, where $B_i(\mathbf{I})$ is the hazard rate function for tipping element i ,
 480 depending on whether other tipping elements have tipped. A general formula for the hazard
 481 rate function is given by

$$482 \quad B_i(\mathbf{I}) = b_i \cdot (1 + \sum_j (I_j \cdot f_{ij})). \quad (3)$$

483 We calibrated the values for b_i using the expert opinions reported in Kriegler et al.⁸ and our
484 previously described methodology¹⁰. Specifically, we calibrated b_i to match the average
485 expert’s cumulative trigger probabilities for each tipping element by the year 2200 for the
486 medium temperature corridor in Kriegler et al.⁸, which implies 2.5 °C warming in 2100 and 3
487 °C warming in 2200. These probabilities are 22% for AMOC, 52% for GIS, 34% for WAIS,
488 48% for AMAZ and 19% for ENSO. The corresponding values for b_i are $b_{AMOC} =$
489 0.00063064 , $b_{GIS} = 0.00188445$, $b_{WAIS} = 0.00103854$, $b_{AMAZ} = 0.00163443$ and $b_{ENSO} =$
490 0.000526678 (Table 1).

491 To model the interaction component of tipping point likelihood, we introduce f_{ij} as an
492 additional probability factor, which describes by how much the hazard factor for tipping
493 element j is affected if tipping element i has tipped (when it is negative, it implies a decrease
494 in probability). The parameter matrix f_{ij} is calibrated for $i, j \in \{AMOC, GIS, WAIS,$
495 $AMAZ, ENSO\}$. Again we use the results in Kriegler et al.⁸ as the source for our calibration
496 of the interaction effects between tipping elements. In particular, we consider the core
497 experts’ assessment of the interaction effects for the “medium” temperature corridor. Our aim
498 is to implement the interactions as direct, conditional alterations to the hazard rate of
499 individual tipping events. Supplementary Table 1 summarizes our calibrated factors, f_{ij} . For
500 some of the interaction effects, experts assessed ambiguous effects. For example, in the case
501 of WAIS affecting AMOC the interaction factor ranges between <0 and >0 among the
502 experts and among the average optimistic and pessimistic opinions of the core experts. In
503 such an ambiguous case, while it might be worthwhile incorporating this uncertainty in the
504 direction of interaction, we leave that as a possible avenue for further research and focus
505 here, as in the non-ambiguous cases, solely on the average core experts’ assessment.

506 The order of the tipping sequence is important for the overall impact of any individual tipping
507 element, due to asymmetric causal relationships between some of the tipping events (Fig. 1,
508 Supplementary Table 1). For example, when GIS tipping is triggered first, the likelihood of
509 AMOC is increased, but if instead a tipping point in the AMOC is triggered first, the
510 likelihood of GIS tipping is reduced.

511

512 **Specification of transition times, final damages, and carbon cycle effects**

513 In addition to calibrating the hazard rate (described above), we have to specify the transition
514 time, final damage levels and the effect on the carbon cycle for each tipping element (Table
515 1). We base this on reviews of the literature, updated from previous work^{7,11}. Recognising the
516 scientific and economic uncertainties in these choices, the transition times are given a
517 common factor of 5 range of uncertainty in either direction from default values, and the final
518 damages are given a factor of 2-3 total uncertainty range. The values chosen are briefly
519 justified as follows:

520 **AMOC:** Past abrupt climate changes linked to reorganisations of the AMOC have occurred in
521 a decade or less, but future AMOC collapse in model simulations can take a couple of
522 centuries. Hence we opt for a 50-year default transition time and 10-250 year range. The
523 AMOC collapse is often viewed as the archetype of a climate catastrophe; hence we assign it
524 the highest final damage (accepting that others will question this). Past studies with DICE
525 have suggested a collapse of the AMOC might result in a 25-30% reduction in GDP
526 comparable with the Great Depression^{27,28}. However, when combined with other tipping
527 events this could lead to excessively high damages, so we opt for a 15% GDP reduction with a
528 range of 10-20%. We considered the potential for the AMOC collapse to reduce both ocean

529 heat⁴⁸ and carbon^{49,50} uptake. However quantitative estimates of these effects based on
530 existing studies⁴⁸⁻⁵⁰ suggest they are small, hence they are ignored here.

531 **GIS:** Irreversible meltdown of the Greenland ice sheet typically takes millennia in model
532 simulations^{51,52}, but models are unable to explain the speed of recent ice loss⁷. To cover the
533 uncertainty we opt for a default timescale of 1500 years, with a minimum timescale⁷ of 300
534 years and an upper limit of 7500 years. The final damages from the GIS melt will largely be
535 due to sea-level rise⁷ of around 7 metres, which is roughly twice what can come from WAIS
536 disintegration⁵³. Hence we give the GIS twice the default final damages of the WAIS, noting
537 that the spatial pattern of sea level rise will be greatest furthest away from each ice sheet (due
538 to gravitational effects). As well as flooding low-lying cities and agricultural land, flooding of
539 large areas of low-lying permafrost (especially in Siberia) could ultimately release large
540 amounts of carbon¹¹. We conservatively assume an exogenous emission of 100 GtC over the
541 duration of the transition, which is only ~6% of the total permafrost carbon reservoir⁵⁴.

542 **WAIS:** The West Antarctic ice sheet is grounded largely below sea level and has the potential
543 for more rapid disintegration than the Greenland ice sheet⁷, ultimately leading to up to 3.3
544 metres sea-level rise⁵³. Past sea-level rise in the penultimate Eemian inter-glacial period is
545 estimated to have occurred⁵⁵ at rates >1 m/century and must have come from Antarctica
546 and/or Greenland. We assign a minimum timescale of 100 years for WAIS disintegration,
547 with a default setting of 500 years, and an upper limit of 2500 years. Noting that the effect of
548 GIS meltdown on Arctic sea level is greatly suppressed by gravitational adjustment⁵⁶,
549 whereas that of WAIS disintegration is not⁵³, we assign WAIS the same potential to release
550 100 GtC from low-lying permafrost over the duration of the transition.

551 **AMAZ:** Dieback of the Amazon rainforest in future model simulations⁵⁷ takes around 50
552 years, which we use as our default. However, if drought and corresponding fires respond very

553 non-linearly to climate change⁵⁸ dieback could conceivably occur on a minimum timescale of
554 10 years, whereas if the forest is more resilient it could take centuries, consistent with a
555 maximum timescale of 250 years. The Amazon rainforest is estimated to store 150-200 GtC
556 in living biomass and soils⁵⁹ and we conservatively assume that dieback will release 50 GtC
557 over the duration of the transition.

558 **ENSO:** In the past the frequency and amplitude of ENSO variability has changed on decadal
559 to centennial timescales⁷, and in the future the amplitude of ENSO variability is expected to
560 increase with more frequent extreme El Niño and extreme La Niña events⁶⁰. Past El Niño and
561 La Niña events have had large impacts, especially on the agricultural sector, and their more
562 global footprint than Amazon dieback leads us to assign higher damages to ENSO. The
563 observational record shows that individual strong El Niño events can cause anomalous
564 emissions of carbon by fire⁶¹ of ~2 GtC. Hence we assume that an increase in El Niño
565 amplitude could readily cause an average increase in land carbon emissions (exogenous) by
566 0.2 GtC/yr that is essentially permanent on the timescale of our integrations.

567 The combined effect on final damages if all tipping points occur is 38%, with a 23%-50%
568 range in our sensitivity analysis. However, the timescale for all damages to be felt in our
569 default case is over 1000 years, and our tipping probabilities are relatively low. Only two
570 tipping elements (GIS, AMAZ) have an expected tipping time around 2200 (when it is as
571 likely as not that their tipping process will be triggered), with the remaining three elements
572 being less likely to tip. Furthermore, slow transition times mean that damages tend to be
573 discounted away. As we have shown previously¹⁰, a tipping point with 2.5% damage to GDP
574 and a 5 year transition time will have much larger impact on the SCC today than a tipping
575 point with 25% damage to GDP and a 500 year transition time. Other integrated assessment
576 model studies that treat tipping points have tended to assume instantaneous transitions and
577 double-digit percentage damages. Thus, we argue that overall our model is conservatively

578 calibrated with relatively low expected damages, which amount to 0.53% of GDP in 2100
 579 and 1.89% of GDP in 2200 in our default model parameterization.

580 The couplings to the carbon cycle lead to the following new specification of the exogenous
 581 land carbon source (in GtC) in DSICE:

$$\begin{aligned}
 582 \quad E_{Land,t} = & 0.9e^{-0.04t} + I_{GIS} \cdot I_{\{J_{GIS} < \overline{J_{GIS}}\}} \cdot \frac{100}{1500} \\
 583 & + I_{WAIS} \cdot I_{\{J_{WAIS} < \overline{J_{WAIS}}\}} \cdot \frac{100}{500} \\
 584 & + I_{AMAZ} \cdot I_{\{J_{AMAZ} < \overline{J_{AMAZ}}\}} \cdot \frac{50}{50} \\
 585 & + 0.2 \left(J_{ENSO} / \overline{J_{ENSO}} \right), \tag{4}
 \end{aligned}$$

586 where the first term on the right hand side is from the DICE model and all remaining terms
 587 are our modifications. Here, $I_{\{\}}$ serves as an indicator function.

588

589 **The Dynamic Programming Problem**

590 In the following we present the dynamic programming problem of the social planner:

$$591 \quad V_t(\mathcal{S}) = \max_{C_t, \mu_t} u(C_t, L_t) + \beta \left[\mathbb{E} \left\{ \left(V_{t+1}(\mathcal{S}^+) \right)^{\frac{1-\gamma}{1-1/\psi}} \right\}^{\frac{1-1/\psi}{1-\gamma}} \right] \tag{5}$$

$$592 \quad s. t \quad K^+ = (1 - \delta)K + Y_t(K, T^{AT}, \mathbf{I}, \mathbf{J}) - C_t - \Psi_t \tag{6}$$

$$593 \quad \mathbf{M}^+ = \Phi^M \mathbf{M} + (\mathcal{E}_t(K, \mu), 0, 0)^\top \tag{7}$$

$$594 \quad \mathbf{T}^+ = \Phi^T \mathbf{T} + (\xi_1 \mathcal{F}_t(M^{AT}), 0)^\top \tag{8}$$

$$595 \quad I_i^+ = g_i(\mathbf{I}, T^{AT}, \omega_i) \tag{9}$$

$$J_i^+ = \min\{J_i + \Delta_i, \bar{J}_i\}I_i \quad (10)$$

597 where $V_t(\mathcal{S})$ denotes the time t value function which is endogenous in the 16-dimensional
598 state vector denoted by \mathcal{S} . Furthermore, C_t, μ_t are the control variables for consumption and
599 mitigation. Each period's utility u depends on consumption and exogenous labour supply L_t .
600 With β we denote the utility discount rate. The expectation operator is over the next-period's
601 value function with γ and ψ denoting the risk aversion parameter and the elasticity of inter-
602 temporal substitution, respectively. In our default parameter case, we follow the calibration
603 by Pindyck & Wang²³ and specify: $\gamma = 3.066$ and $\psi = 1.5$. Furthermore, K, \mathbf{M} and \mathbf{T} denote
604 the capital stock, the three carbon stocks and the two temperatures (M^{AT} and T^{AT} represent
605 carbon concentration and temperature in the atmosphere), respectively and a “+” superscript
606 denotes a variable's next period value. Y_t denotes world gross product net of damages and \mathcal{E}_t
607 denotes non-mitigated emissions into the atmosphere. Finally Ψ_t is the expenditure on
608 mitigation, and \mathcal{F}_t is a term related to radiative forcing. The model is solved for the next 300
609 years with a terminal value function approximating the welfare of future years from 301 to
610 infinite horizon (see Supplementary Methods). Our SCC is computed via

$$611 \quad SCC_t = -1000 \left(\frac{\partial V_t}{\partial M_t^{AT}} \right) / \left(\frac{\partial V_t}{\partial K_t} \right),$$

612 as in DSICE¹⁹, denoting the marginal rate of substitution between atmospheric carbon
613 concentration and capital.

614 After solving the dynamic programming problem using parallel backward value function
615 iteration⁴⁶ (see Supplementary Methods), we use these approximated value functions V_t to
616 simulate 10,000 paths in the following way: at the initial time, its state vector \mathcal{S}_0 is known as
617 the observed market values, then we can get the optimal consumption and emission control
618 rate at time 0 by solving the dynamic programming problem with the previously computed

619 V_1 . Using sample realization of shocks, we can obtain the next state vector \mathcal{S}_1 ; using the same
620 method to iterate forward, we get one simulated path of states and optimal policies that
621 depend on realization of shocks. Repeating this process, we get 10,000 sample paths for our
622 analysis.

623

624 **Numerical Implementation of the Model**

625 We have found that for the relatively short time horizon, when recalibrating the carbon cycle
626 and temperature modules to match all four RCP scenarios closely we can omit the deep ocean
627 stock of carbon without any loss of accuracy in the carbon-to-temperature relationship. Thus,
628 the numerical implementation of the model is fifteen-dimensional. The computational task
629 required to solve this fifteen-dimensional problem goes far beyond what has previously been
630 achieved in truly stochastic climate-economy models, where 3-4 dimensional problems are
631 considered the current frontier. We solve the model with parallel dynamic programming
632 methods⁴⁶ on 312,500,000 approximation nodes for the 10-dimensional continuous state
633 space and degree-4 complete Chebyshev polynomials for each of the 5 discrete state vectors.
634 It takes about 3 hours to solve the model for a single set of parameter values on 10,560 cores
635 at the Blue Waters supercomputer. The estimated error bound of the optimal solution is 0.1%-
636 1% for policy functions and 0.01%-0.1% for the value functions.

637

638 **Sensitivity analyses**

639 We conducted several sensitivity analyses. Firstly we varied the transition times and/or
640 damages of all five tipping elements across their assigned uncertainty ranges. Secondly we

641 took a more pessimistic assessment of the interaction between the tipping elements
642 (Supplementary Table 3), which uses the upper bounds of the core experts' assessment.

643 Thirdly, some more complex sensitivity studies were also conducted exploring the effect of
644 endogenous transition times for tipping elements. In our model the transition time for tipping
645 element i is inversely tied to $\Delta_{i,t}$, the annual damage increase during the transition phase.

646 Thus, the transition time for element i is proportional to $\frac{1}{\Delta_{i,t}}$ and also its final damage level \bar{J}_i .

647 In the case of an endogenous transition time, we let the annual damage increase be $\Delta_{i,t} =$
648 $\bar{J}_i \exp(a_i T_t^{AT} - b_i)$, where a_i and b_i are parameters calibrated to result in $\bar{J}_i / \Delta_{i,t}$ to be the
649 long transition time for $T_t^{AT} = 0$ and short transition time for $T_t^{AT} = 6$. Thus, the endogenous
650 transition time is equal to $\int_0^\infty \exp(a_i T_t^{AT} - b_i) I_{i,t} I_{-}(J_{i,t} < \bar{J}_i) dt$.

651 As a general rule, transition timescales should be governed by the internal dynamical
652 timescale(s) of the system in question, so it may not be appropriate to include a temperature
653 dependence of the transition timescale for all tipping elements. However, endogenous
654 transition times have some backing for the major ice sheets, where models^{51,52}, show that the
655 rate of ice sheet meltdown depends on the amount by which a temperature threshold is
656 exceeded.

657

658 **Additional References**

- 659 46 Cai, Y., Judd, K.L., Thain, G., & Wright, S.J., Solving Dynamic Programming
660 Problems on a Computational Grid. *Comput. Econ.* 45 (2), 261-284 (2015).
- 661 47 E. Nævdal, E. & Oppenheimer, M., The Economics of the Thermohaline Circulation
662 – A Problem with Multiple Thresholds of Unknown Location. *Resource and Energy*

663 *Economics* 29, 4:262–283 (2007).

664 48 Kostov, Y., Armour, K.C., & Marshall, J., Impact of the Atlantic meridional
665 overturning circulation on ocean heat storage and transient climate change.
666 *Geophysical Research Letters* 41 (6), 2108-2116 (2014).

667 49 Perez, F.F. *et al.*, Atlantic Ocean CO₂ uptake reduced by weakening of the meridional
668 overturning circulation. *Nature Geosci* 6 (2), 146-152 (2013).

669 50 Zickfeld, K., Eby, M., & Weaver, A.J., Carbon-cycle feedbacks of changes in the
670 Atlantic meridional overturning circulation under future atmospheric CO₂. *Global*
671 *Biogeochemical Cycles* 22 (3), GB3024 (2008).

672 51 Huybrechts, P. & De Wolde, J., The Dynamic Response of the Greenland and
673 Antarctic Ice Sheets to Multiple-Century Climatic Warming. *Journal of Climate* 12,
674 2169-2188 (1999).

675 52 Robinson, A., Calov, R., & Ganopolski, A., Multistability and critical thresholds of
676 the Greenland ice sheet. *Nature Clim. Change* 2 (6), 429-432 (2012).

677 53 Bamber, J.L., Riva, R.E.M., Vermeersen, B.L.A., & LeBrocq, A.M., Reassessment of
678 the Potential Sea-Level Rise from a Collapse of the West Antarctic Ice Sheet. *Science*
679 324 (5929), 901-903 (2009).

680 54 Tarnocai, C. *et al.*, Soil organic carbon pools in the northern circumpolar permafrost
681 region. *Global Biogeochemical Cycles* 23 (2), GB2023 (2009).

682 55 Rohling, E.J. *et al.*, High rates of sea-level rise during the last interglacial period.
683 *Nature Geoscience* 1, 38-42 (2008).

684 56 Mitrovica, J.X., Tamislea, M.E., Davis, J.L., & Milne, G.A., Recent mass balance of
685 polar ice sheets inferred from patterns of sea-level change. *Nature* 409, 1026-1029
686 (2001).

687 57 Huntingford, C. *et al.*, Towards quantifying uncertainty in predictions of Amazon
688 ‘dieback’. *Philosophical Transactions of the Royal Society of London B: Biological*
689 *Sciences* 363 (1498), 1857-1864 (2008).

690 58 Brando, P.M. *et al.*, Abrupt increases in Amazonian tree mortality due to drought–fire
691 interactions. *Proceedings of the National Academy of Sciences* 111 (17), 6347-6352
692 (2014).

693 59 Feldpausch, T.R. *et al.*, Tree height integrated into pantropical forest biomass
694 estimates. *Biogeosciences* 9 (8), 3381-3403 (2012).

695 60 Cai, W. *et al.*, ENSO and greenhouse warming. *Nature Clim. Change* 5 (9), 849-859
696 (2015).

697 61 van der Werf, G.R. *et al.*, Continental-Scale Partitioning of Fire Emissions During the
698 1997 to 2001 El Niño/La Niña Period. *Science* 303 (5654), 73-76 (2004).

699

700

701 **Supplementary Information:**

702

703 **Supplementary Methods: Calibration for the Climate System**

704 The DSICE model used in this study is based on the DICE-2013R model where the carbon
705 cycle and temperature modules are represented by a three-box and a two-box model
706 respectively. DICE-2013R uses five-year time steps and its carbon cycle and temperature
707 modules are calibrated with one RCP scenario. Our DSICE model instead uses annual time
708 steps and four RCP scenarios (RCP2.6, RCP4.5, RCP6, RCP8.5) to calibrate the parameters
709 in the carbon cycle and temperature modules. For each RCP emission scenario, MAGICC
710 provides their corresponding scenarios of carbon concentration and temperature in the
711 atmosphere. We use this information to calibrate the parameters in our carbon cycle and
712 temperature modules.

713 For each RCP emission scenario, we first use it as the input E_t to the carbon cycle, and then it
714 outputs a path of carbon concentration in the atmosphere via

$$\mathbf{M}_{t+1} = \Phi^M \mathbf{M}_t + (E_t, 0, 0)^\top$$

715 with the carbon cycle transition matrix

$$\Phi^M = \begin{bmatrix} 1 - \phi_{12} & \phi_{12} & 0 \\ \phi_{12} & 1 - \phi_{21} - \phi_{23} & \phi_{32} \\ 0 & \phi_{23} & 1 - \phi_{32} \end{bmatrix}$$

716 We calibrate the parameters in Φ^M so that our generated paths of carbon concentration in the
717 atmosphere match their corresponding RCP scenarios of carbon concentration in the
718 atmosphere for all four RCP scenarios. Our numerical calibration shows that ϕ_{23} and ϕ_{32} are

719 nearly zero, so we drop the carbon concentration in the deep ocean in our numerical
 720 implementation, and find that it has almost no impact on the solutions.

721 The carbon concentrations in the atmosphere generate radiative forcing:

$$722 \quad F_t = \eta \log_2(M^{AT}/M_*^{AT}) + F_t^{EX},$$

723 where M_*^{AT} is the preindustrial carbon concentration in the atmosphere, and F_t^{EX} is exogenous
 724 radiative forcing. The radiative forcing impacts the surface temperature. With our carbon
 725 concentration paths, we have their corresponding radiative forcing scenarios. Using each of
 726 them as the input to the temperature system

$$727 \quad \mathbf{T}_{t+1} = \mathbf{\Phi}^T \mathbf{T}_t + (\xi_1 F_t, 0)^T,$$

728 with

$$729 \quad \mathbf{\Phi}^T = \begin{bmatrix} 1 - \varphi_{21} - \xi_2 & \varphi_{21} \\ \varphi_{12} & 1 - \varphi_{12} \end{bmatrix},$$

730 we can generate one path of surface temperature. We calibrate the parameters ξ_1 , ξ_2 , φ_{21} , φ_{12}
 731 so that our generated paths of surface temperature match the corresponding RCP scenarios of
 732 surface temperature for all four RCP scenarios.

733

734 **Supplementary Methods: Economic System**

735 In the economic system of DSICE, our utility at period t is

$$736 \quad u(C_t, L_t) = \frac{(C_t/L_t)^{1-1/\psi}}{1-1/\psi} L_t,$$

737 where C_t is consumption, ψ is IES (inter-temporal elasticity of substitution), and L_t is
 738 population (in billions) given as

$$L_t = 6.838e^{-0.0254t} + 10.5(1 - e^{-0.0254t})$$

739 The gross world output at year t is

$$Y_t(K_t, T_t^{AT}, \mathbf{I}_t, \mathbf{J}_t) = A_t K_t^\alpha L_t^{1-\alpha} \Omega_t(T_t^{AT}, \mathbf{J}_t, \mathbf{I}_t)$$

740 with

$$\Omega_t(T_t^{AT}, \mathbf{J}_t, \mathbf{I}_t) = \frac{\prod_i (1 - I_{i,t} J_{i,t})}{1 + \pi_2 (T_t^{AT})^2}$$

741 defined in the main text. The mitigation expenditure is

$$\Psi_t = \theta_{1,t} \mu_t^{\theta_2} Y_t(K_t, T_t^{AT}, \mathbf{I}_t, \mathbf{J}_t)$$

742 Thus, the law of transition for capital K_t is

$$K_{t+1} = (1 - \delta)K_t + Y_t(K_t, T_t^{AT}, \mathbf{I}_t, \mathbf{J}_t) - C_t - \Psi_t$$

743 The carbon emission from economic activity and land is

$$\mathcal{E}_t(K_t, \mu_t) = \sigma_t (1 - \mu_t) A_t K_t^\alpha L_t^{1-\alpha} + E_t^{Land}$$

744 where E_t^{Land} is defined in the main text. The exogenous paths A_t , $\theta_{1,t}$, σ_t , and the parameter

745 values for α , π_2 , θ_2 , δ follow DICE-2013R.

746

747 **Supplementary Methods: Terminal Value Function**

748 Welfare is usually defined over an infinite horizon, while DICE-2013R approximates it with

749 a 300 years horizon for numerical implementation, as values after 300 years are discounted to

750 be small. In the DSICE model, we use a terminal value function at the “terminal” time $t=301$

751 to approximate the welfare after 300 years, for a more precise numerical implementation and

752 also a more stable value function iteration for solving the dynamic programming problem
753 defined in the main text.

754 To compute the terminal value function, we assume that the emission control rate will always
755 be one after 300 years, and consumption will always be 0.74 share of gross world production.
756 If one tipping element has been tipped before the terminal time, then its damage will keep
757 unfolding, otherwise we assume it will never be tipped after the terminal time. We assume
758 that all exogenous paths will stop changing after the terminal time. Under these assumptions,
759 for any terminal state \mathcal{S} , we can generate a flow of consumption after the terminal time, and
760 then we estimate the value of the terminal value function at that state to be

$$V_{301}(\mathcal{S}) = \sum_{t=301}^{\infty} e^{-\rho(t-301)} u(C_t, L_t)$$

761 For the numerical implementation, we compute the above summation over 400 years (i.e.,
762 from year 301 to 700) as an approximation. Our numerical examples show that solutions for
763 the first 200 years are insensitive to the choice of the terminal value function, due to the
764 discounted effect inherent in the DICE-2013R model, but the terminal value function
765 specified above is still essential because it enables us to have stable value function iteration.

766

767 **Supplementary Methods: The Numerical Algorithm**

768 We use parallel backward value function iteration⁴⁶ to solve the dynamic programming
769 problem (5)-(10). With the above defined terminal value function V_{301} , for a state \mathcal{S} at time
770 $t=300$, we use an optimization solver to solve the dynamic programming problem and then
771 get $V_{300}(\mathcal{S})$. Since this is a problem with both continuous and discrete state variables, we
772 cannot compute $V_{300}(\mathcal{S})$ for all possible states \mathcal{S} . Instead we choose a set of approximation

773 state nodes \mathcal{S}_i and compute $v_i = V_{300}(\mathcal{S}_i)$, and then use a complete Chebyshev polynomial to
774 approximate the value function V_{300} at continuous state variables for each discrete state
775 vector, so that $v_i \approx V_{300}(\mathcal{S}_i)$, but now we have a value of V_{300} at any state \mathcal{S} . Note that these
776 optimization problems are naturally parallelizable. Iterating backwards from $t=300$ to $t=0$, we
777 get all value functions V_t and also their corresponding policy functions. Using these value
778 functions, we can then iterate forward to get one simulated path of optimal policies which
779 depend on realization of the shocks, and repeat it to obtain 10,000 simulation paths, as
780 described in the main text. See refs. ^{19,46} for more detailed discussion.

781

782

783

784

785

786

787

788

789

790

791

792

793

794 **Supplementary Tables**

795

796 **Supplementary Table 1.** Interaction terms between tipping events (f_{ij}), which describe by
 797 how much the hazard factor for tipping element j is affected if tipping element i has tipped.

Tipping element i	Tipping element j				
	AMOC	GIS	WAIS	AMAZ	ENSO
AMOC		-0.235	0.125	0.55	0.121
GIS	1.62		0.378	0.108	0
WAIS	0.107	0.246		0	0
AMAZ	0	0	0		0
ENSO	-0.083	0	0.5	2.059	

798

799

800 **Supplementary Table 2.** Sensitivity analysis for simultaneously varying the transition times
 801 and damages of all five tipping elements.

Social cost of carbon in 2010 (\$/tCO ₂)	High damage	Default damage	Low damage
Short transition time	166	145	94
Default transition time	145	116	77
Long transition time	75	62	50

802

803

804 **Supplementary Table 3.** Pessimistic assessment of the interaction terms between tipping
 805 events (f_{ij}) using the upper bounds of the core experts' assessment.

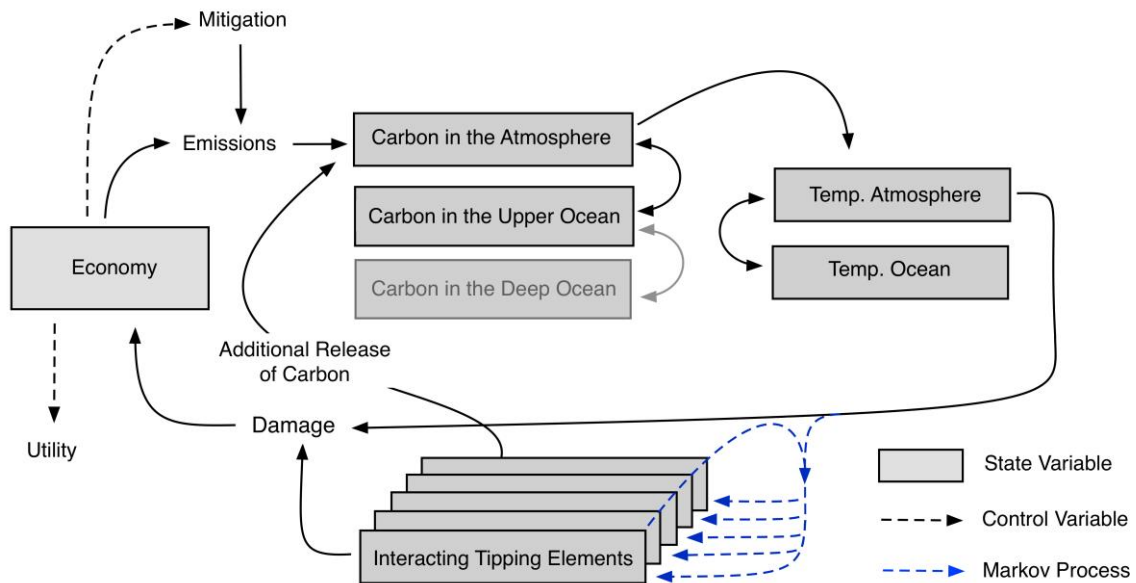
Tipping element i	Tipping element j				
	AMOC	GIS	WAIS	AMAZ	ENSO
AMOC		-0.056	0.25	1	0.25
GIS	3.04		0.68	0.2	0
WAIS	0.44	0.483		0	0
AMAZ	0	0	0		0
ENSO	0.16	0	1	3.83	

806

807

808

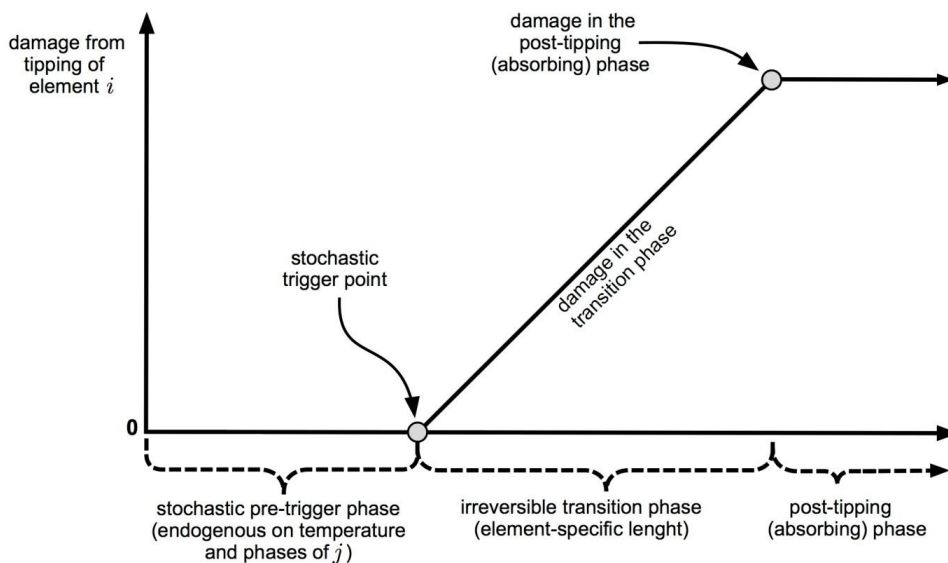
809 **Supplementary Figures**



810

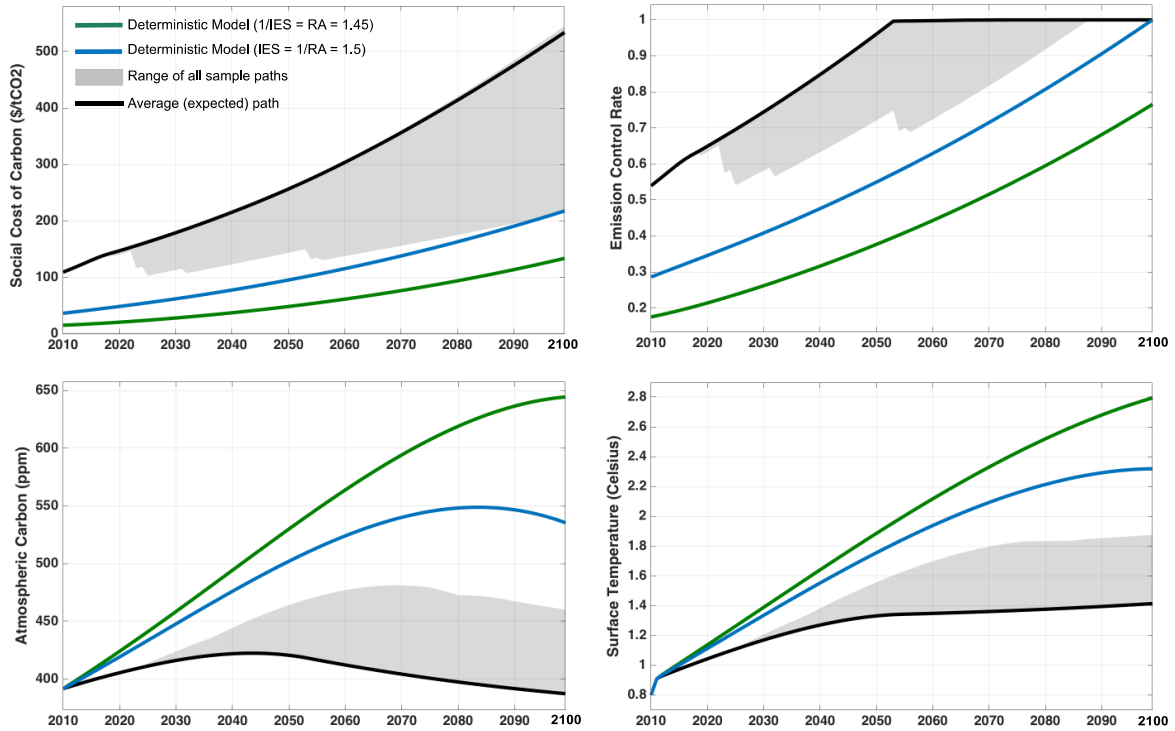
811 **Supplementary Figure 1.** Schematic of the DSICE model used in this study. The “deep
 812 ocean carbon” box is shaded as it can be omitted in the numerical analysis (see “Numerical
 813 Implementation of the Model” in the Methods section).

814



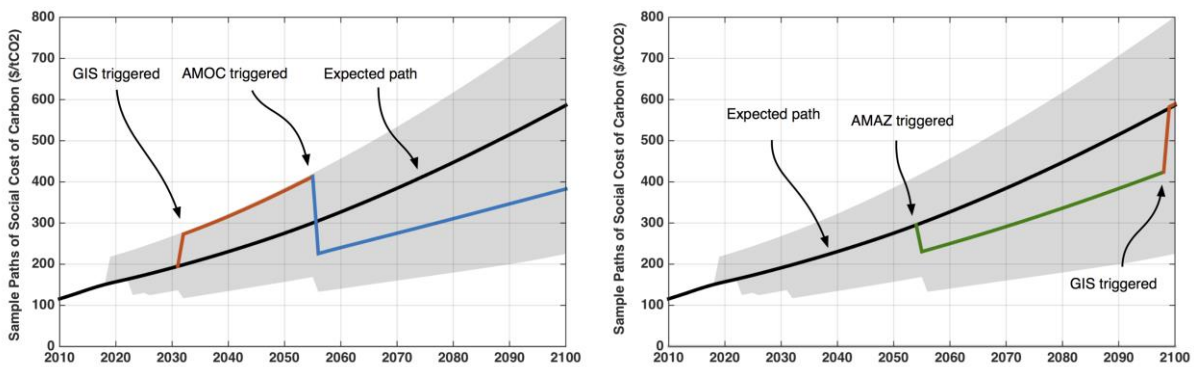
815

816 **Supplementary Figure 2.** Schematic of the tipping process in the DSICE model.



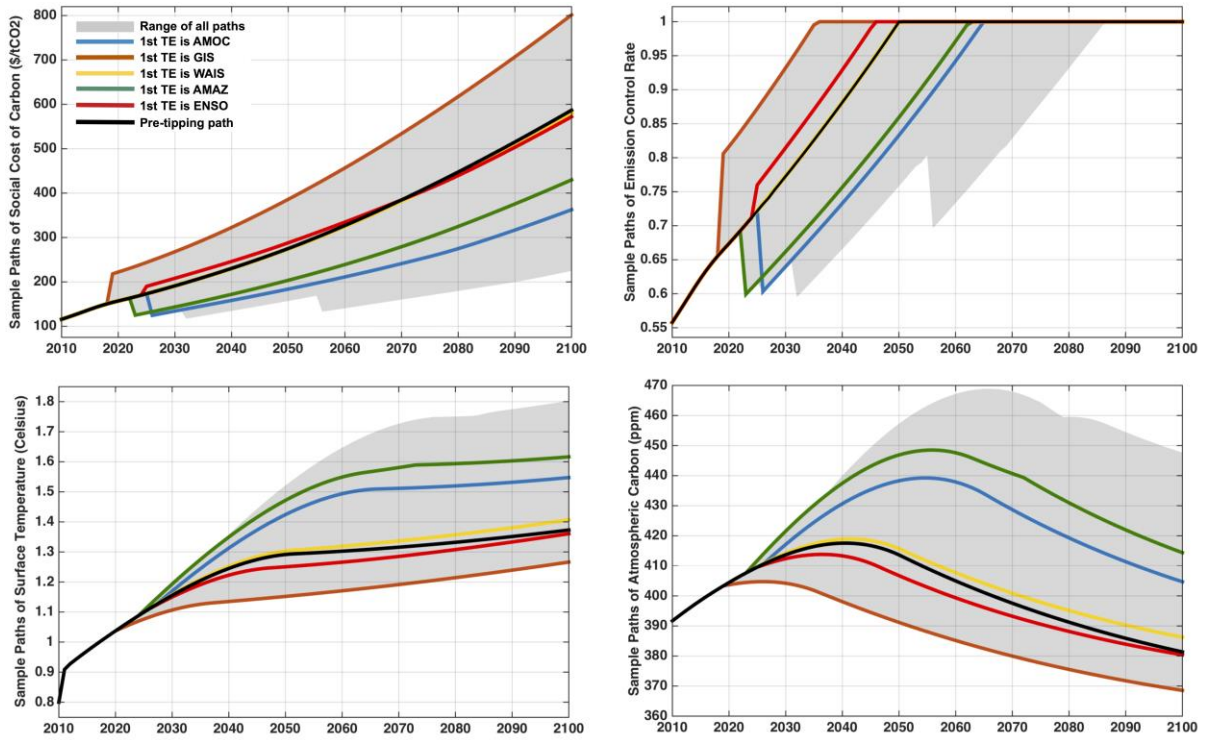
817

818 **Supplementary Figure 3.** Results for: (a) the social cost of carbon, (b) emissions control
 819 policy, (c) atmospheric carbon (ppm), and (d) surface temperature change (above pre-
 820 industrial), in the baseline deterministic model (green), the deterministic model with Epstein-
 821 Zin preferences (blue), and the expected path of stochastic model with multiple tipping points
 822 (black) in case without interaction. The grey-shaded area shows the range of sample paths
 823 from 10,000 simulations of the stochastic model (see Figure 2 for the analogous case with
 824 interaction).



825

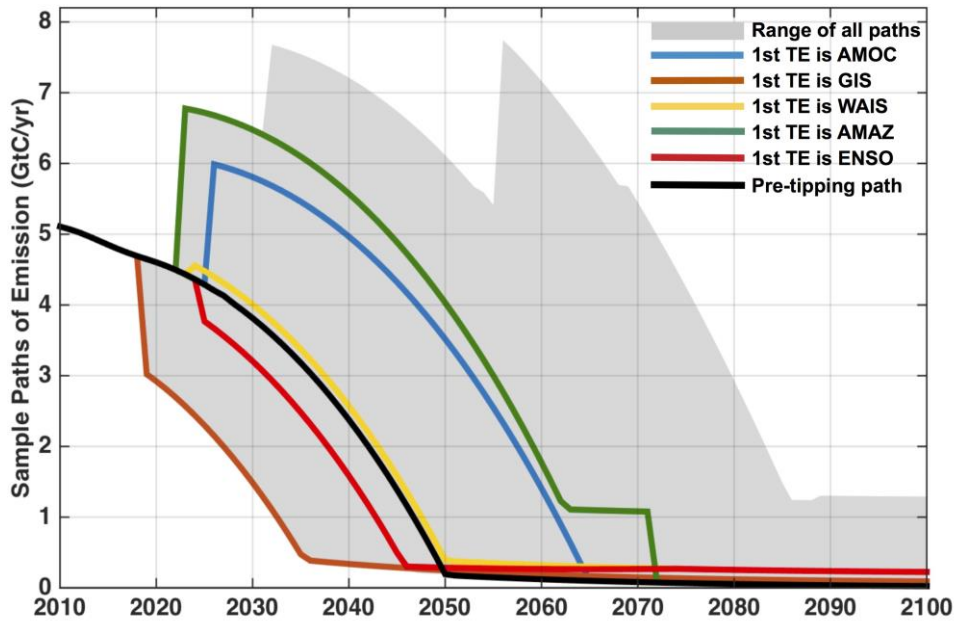
826 **Supplementary Figure 4.** Example sample paths with two tipping events this century.



827

828 **Supplementary Figure 5.** Sample paths of the earliest (and sole) tipping of each element.

829



830

831 **Supplementary Figure 6.** Sample emission paths of the earliest (and sole) tipping of each
832 element.

833

834